Electronic Supplementary Material (ESI) for Journal of Materials Chemistry A.

Supplementary Material

Nitrogen-doped amorphous/graphitic hybrid carbon material derived from sustainable resource for low-cost K-ion battery anode

Yeseul Jeong,[1,#] Hyeon-Ji Shin,[2,3,#] Gwangeon Oh,[1] Muhammad Hilmy Alfaruqi,[1] Mohammad Shamsuddin Ahmed,[1] Vinod Mathew,[1] Hun-Gi Jung,[2,3,*] Jaekook Kim,[1,*] Jang-Yeon Hwang[1,*]

[1]Department of Materials Science and Engineering, Chonnam National University, Gwangju 61186, Republic of Korea

[2]Energy Storage Research Center, Clean Energy Research Division, Korea Institute of Science and Technology, Seoul 02792, Republic of Korea

[3]Division of Energy and Environment Technology, KIST School, Korea University of Science and Technology, Seoul 02792, Republic of Korea

Author Information

[#]These authors contribute equally to this work.

Corresponding Author

*E-mail: hungi@kist.re.kr; jaekook@jnu.ac.kr; hjy@jnu.ac.kr

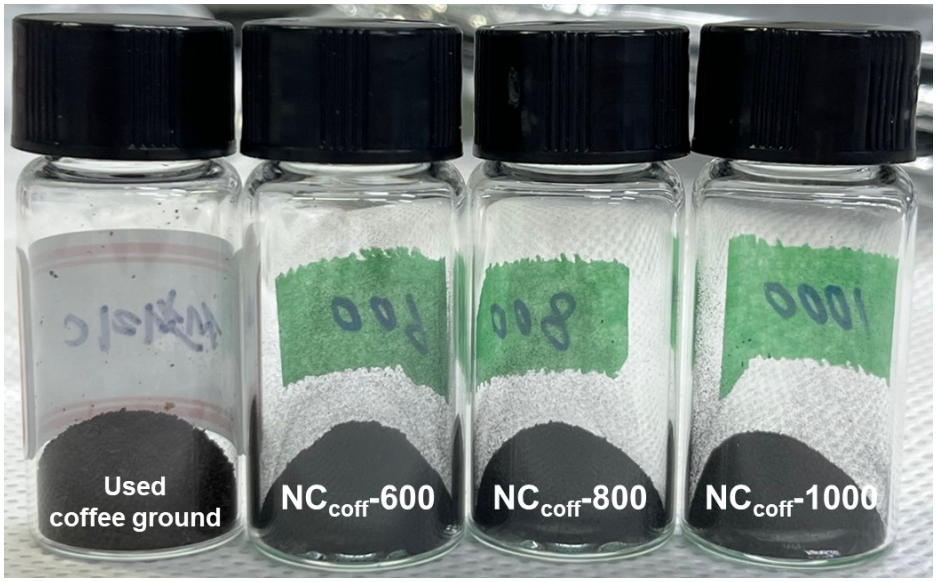

Fig. S1 A comparison photograph of the used coffee ground before / after the pyrolysis process.

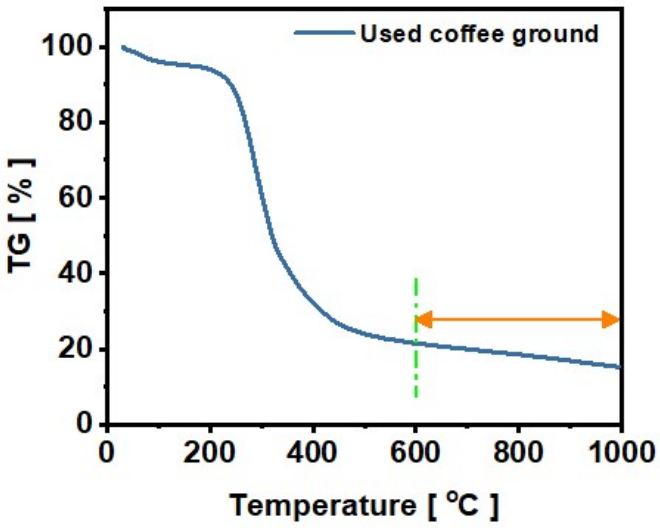

Fig. S2 Thermogravimetric analysis of used coffee ground up to 1000 ℃ under Ar-atmosphere.

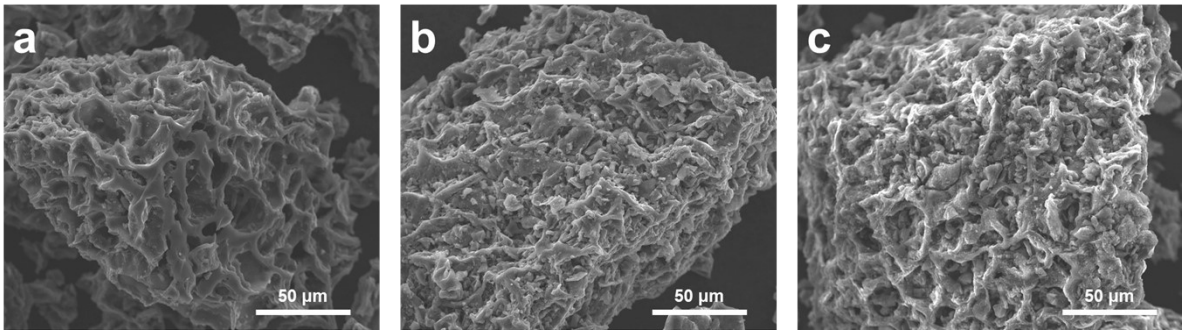

Fig. S3 Low magnification SEM images of (a) NC_{coff}-600, (b) NC_{coff}-800, and (c) NC_{coff}-1000.

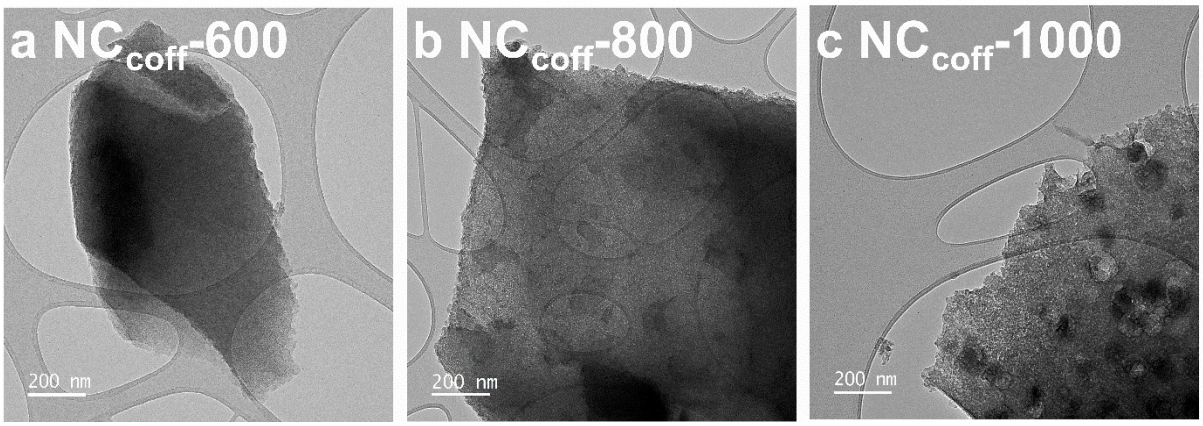

Fig. S4 Transmission electron microscopy (TEM) images of (a) NC_{coff}-600, (b) NC_{coff}-800, and (c) NC_{coff}-1000.

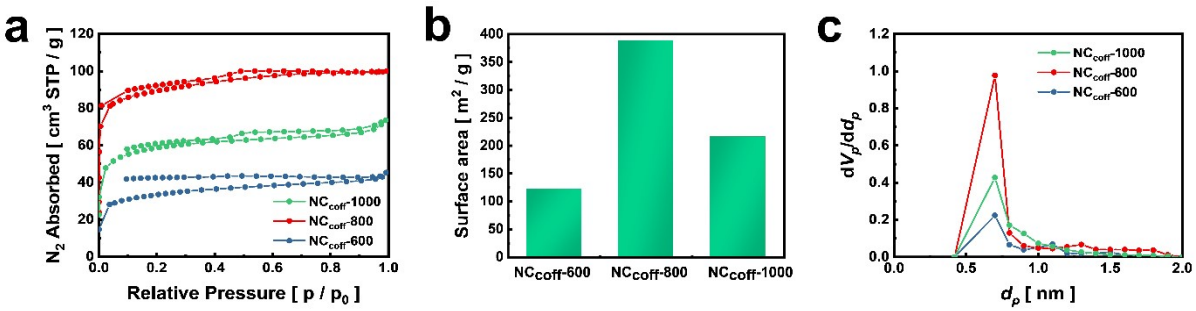

Fig. S5 Comparative (a) N_2-adsorption–desorption isotherms, (b) Brunauer–Emmett–Teller (BET) surface area histograms, and (c) Barrett–Joyner–Halenda (BJH) pore-size distribution plots of NC_{coff}-600, NC_{coff}-800, and NC_{coff}-1000.

Table S1. Surface area and porosity features of the NC_{coff} samples.

Sample	$a_{s, BET}$ ($m^2 g^{-1}$)	Total pore volume (p/p_0 = 0.990) ($cm^3 g^{-1}$)	Micropore volume ($cm^3 g^{-1}$)	Mesopore volume ($cm^3 g^{-1}$)	Micropore size (nm)
NC_{coff}-600	121.39	0.069491	0.057779	0.027397	0.7
NC_{coff}-800	338.65	0.1545	0.1604	0.03079	0.7
NC_{coff}-1000	215.88	0.1134	0.098935	0.033742	0.7

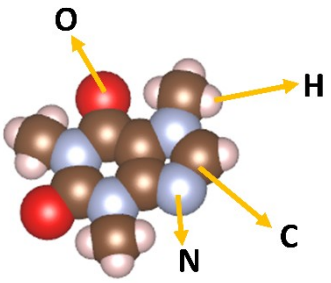

Fig. S6 Chemical structure of caffeine.

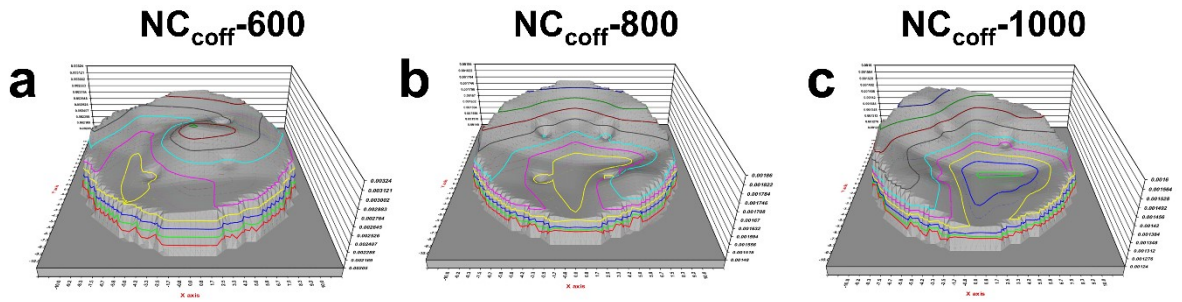

Fig. S7 Electrical conductivity measured via the 4-point probe direct current (DC) method as shown by 3D resistance mapping for three NC_{coff} electrodes.

The resistivity and electrical conductivity of the NC_{coff} electrodes in relation to the heat treatment temperature were measured at 25 °C (room temperature) via the 4-point probe DC method. The resistance of the electrode (diameter: 16 mm), shown on the x–y plane, is presented as a 3D contour line. It was confirmed that the resistance values of each sample were similar across all points, specifically the 3-D contour of (a) NC_{coff}-600, (b) NC_{coff}-800, and (c) NC_{coff}-1000. The x- and y-axes indicate position, and the z-axis indicates resistance. Detailed values of average resistivity and electrical conductivity are summarized in Table S2.

Table S2. Corresponding average resistivity and electrical conductivity depicted in Figure S4.

Sample	Avg (ohm·cm)	Conductivity
NC_{coff}-600	3.23×10^{-5}	3.09×10^{4}
NC_{coff}-800	1.44×10^{-5}	6.96×10^{4}
NC_{coff}-1000	2.19×10^{-5}	4.57×10^{4}

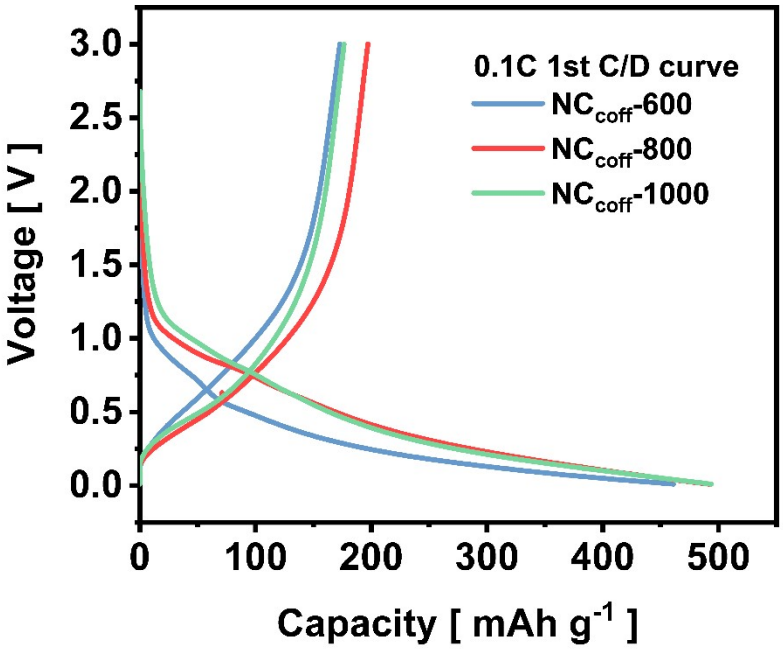

Fig. S8 Charge–discharge voltage profiles of NC_{coff} anode half-cell with the first cycle at 0.1 C in the voltage range of 0.01–3 V (vs. K/K^+).

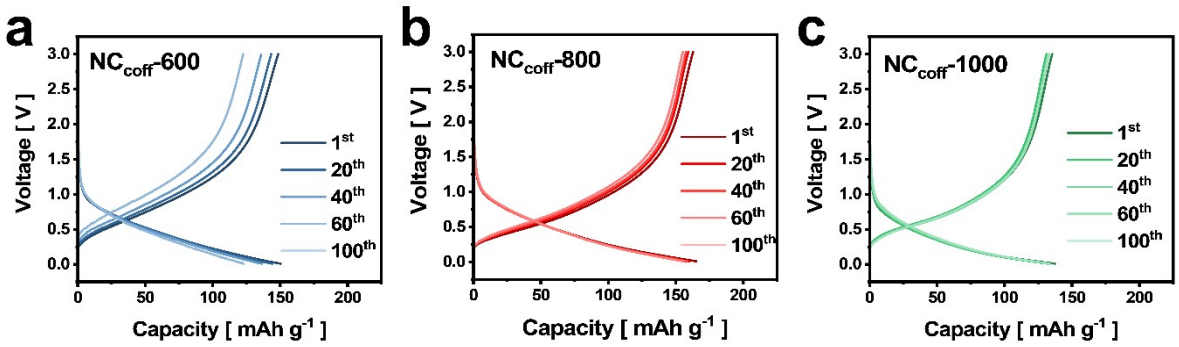

Fig. S9 Charge–discharge voltage profiles of the NC_{coff} anode half-cell with the 1st, 20th, 40th, 60th, and 100th cycle of 0.2 C for (a) NC_{coff}-600, (b) NC_{coff}-800, and (c) NC_{coff}-1000 in the voltage range of 0.01–3 V (vs. K/K^+).

Table S3. The diffusion coefficients (D_{K+}) calculated for the electrodes after 15 cycles.

Sample	**Diffusion coefficient (D_{K^+})**
NC_{coff}-600	0.74 x 10^{-9} cm^2 s^{-1}
NC_{coff}-800	1.19 x 10^{-9} cm^2 s^{-1}
NC_{coff}-1000	0.58 x 10^{-9} cm^2 s^{-1}

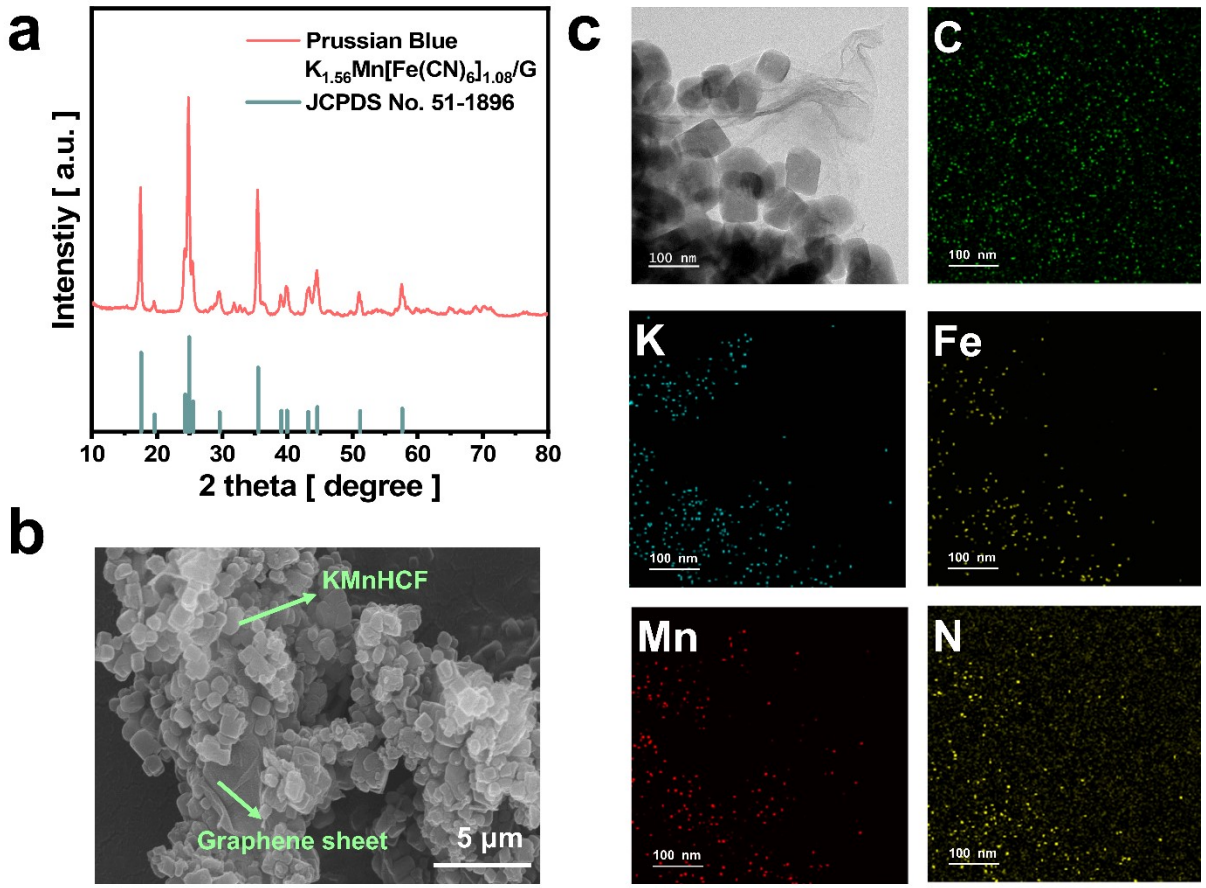

Fig. S10 (a) X-ray diffraction (XRD) results, (b) scanning electron microscopy (SEM) image, and (c) transmission electron microscopy (TEM) image of the synthesized Prussian blue/graphene (PB/G) composite cathode for full-cell measurements and the corresponding energy dispersive X-ray spectroscopy (EDX) mapping images.

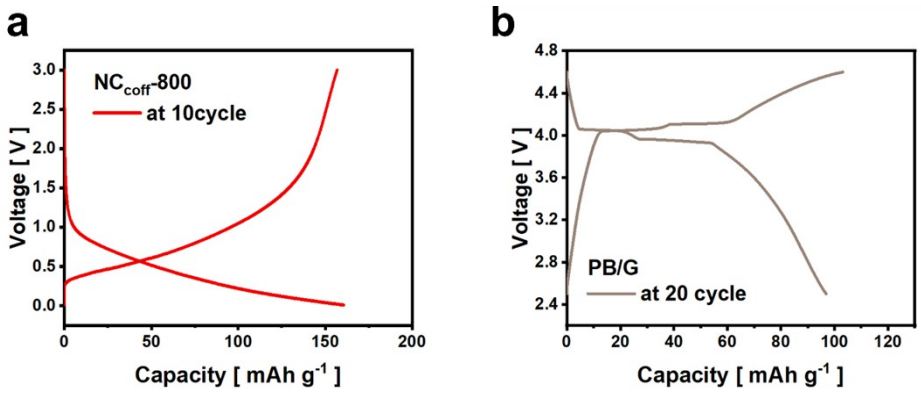

Fig. S11 Charge–discharge voltage profiles tested with (a) NC_{coff}-800 and (b) PB/G half cell at 0.1 C rate for 10 and 20 cycles as pre-cycling prior to configuring the full-cell. The voltage ranges measured for the PB/G cathode and NC_{coff}-800 anode are 2.5–4.6 V (vs. K/K^+) and 0.01–3 V (vs. K/K^+), respectively.

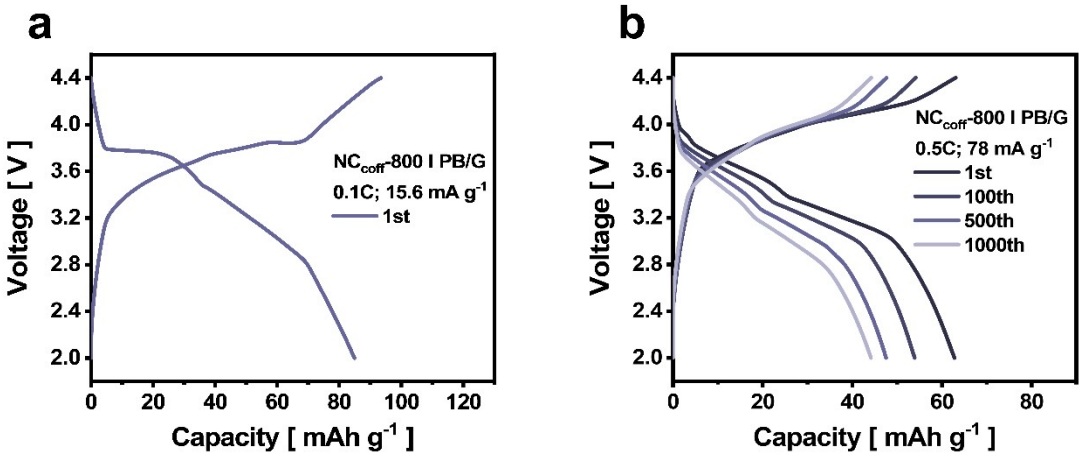

Fig. S12 Charge–discharge voltage profiles of the NC_{coff}-800 | PB/G full-cell with 1st, 100th, 500th, 1000th cycle of 0.5 C in the voltage range 2.0–4.4 V.

Table S4. Summary of biomass-derived carbon for potassium-ion batteries.

Anode materials	Synthesis method	SSA ($m^2 g^{-1}$)	Electrolyte	Current density ($mA g^{-1}$)	Voltage range (V)	Initial capacity ($mAh g^{-1}$)	Capacity retention	Diffusion-controlled reaction from CV (%)	Full cell	Ref.
Used coffee ground	800 ℃ 5h Ar	338.65	0.5 M KPF_6 in EC:DEC (1:1 v/v)	40	0.01 – 3	170.3	90.4 % @ 100 cycles	47 at 15 mV / s	$KMn[Fe(CN)_6]$ / G C. E.; 99.9% @ 1000 cycles	This work
Bamboo charcoal	Activating agent (KOH) + 700 ℃ 2 h at N_2 + sulfur mixture + 700 ℃ 2 h N_2	336.4	0.8 M KPF_6 in EC:DEC (1:1 v/v)	200	0.01 - 3	155	131.5 % @ 300 cycles	N/A	N/A	[1]
Chitin	700 ℃ 2 h Ar	309.45	0.8 M KPF_6 in EC:DEC (1:1 v/v)	56	0.01 – 2	240	86.1% @ 200 cycles	N/A	N/A	[2]
Soybean roots	Activating agent (HCl) + 700℃ 2 h Ar	10.5	0.8 M KPF_6 in EC:DEC (1:1 v/v)	1000	0.01 - 3	330	80 % @ 500 cycles	20.2 at 2 mV / s	N/A	[3]
Potato	1000 ℃ 2 h Ar	531.67	3 M KFSI in DME	100	0.01 – 2.7	270..2	91.7 % @ 100 cycles1	N/A	N/A	[4]
Cyanobacteria	Activating agent (KCl + NaCl) + 800 ℃ 3 h	473.7	0.8 M KPF_6 in EC:DMC (1:1 v/v)	50	0.01 – 3	352	75.6 % @ 100 cycles	N/A	N/A	[5]
Oak	1100 ℃ 6 h Ar	156	0.4 M KPF_6 in EC:DEC (1:1 v/v)	100	0.01 – 3	144.5	93.4 % @ 150 cycles	N/A	N/A	[6]
Loofah	Activating agent (KOH) + 1000 ℃ 2 h N_2	270	1 M KPF_6 in EC:DMC (1:1 v/v)	100	0.01 – 3	155	96.8 % @ 200 cycles	N/A	N/A	[7]
Walnut septum	Urea solution + 800 ℃ 2 h Ar	99.6	0.8 M KPF_6 in EC:DEC (1:1 v/v)	100	0.005 - 3	263.6	92 % @ 200 cycles	17 at 1 mV / s	N/A	[8]
Sugar cane	Activating agent (KOH) + 800 ℃ 2 h N_2 + 900 ℃ 2 h N_2	425.1	0.8 M KPF_6 in EC:DMC (1:1 v/v)	100	0.01 – 2.5	463	65.7 % @ 100 cycles	N/A	N/A	[9]
Artemisia Hedinii	Activating agent (KOH) + 800 ℃ 1 h N_2	1196	0.8 M KPF_6 in EC:DEC (1:1 v/v)	69.75	0.01 – 3	116.4	94.5 % @ 500 cycles	38.2 at 1 mV / s	N/A	[10]
Skimmed cotton	850 ℃ Ar + sulfur mixture	612	1 M KPF_6 in DME	1000	0.01 – 2	194	90.2 % @ 100 cycles	N/A	N/A	[11]
Corn stalks	Urea solution + 275 ℃ 6 h Ar + 1200 ℃ 2 h Ar	130.8	0.8 M KPF_6 in EC:DEC (1:1 v/v)	1000	0.01 – 2.5	200	88 % @ 260 cycles	N/A	N/A	[12]
Chicken bones	Activating agent (HNO_3) 450 ℃ Ar + 850 ℃ 1 h Ar	1474.5	1 M KPF_6 in EC:DEC (1:1 v/v)	58	0.01 - 3	470	43.6 % @ 450 cycles	N/A	N/A	[13]

Skimmed cotton	Activating agent (HCl) + 900 ℃ 2 h Ar + 1200 ℃ 2 h Ar	354	1 M KPF_6 in DME	200	0 – 2.5	240	92 % @ 150 cycles	32 at 1 mV / s	$KFe[Fe(CN)_6]$ C. E.; 97% @ 80 cycles	[14]
Gelatin	800 ℃ 1 h Ar	N/A	1 M KPF_6 in EC:DEC (1:1 v/v)	200	0.01 - 3	92	89.3 % @ 300 cycles	43.3 at 1 mV / s	N/A	[15]
Orange peel	Activating agent (HCl) + 1000 ℃ 2 h N_2 + 350 ℃ 3 h air	113.86	0.8 M KPF_6 in EC:DEC (1:1 v/v)	50	0.01 - 3	320.8	80.9 % @ 150 cycles	N/A	N/A	[16]
Dandelion seed	Activating agent (KOH) + 800 ℃ 2 h Ar	1303	0.8 M KPF_6 in EC:DEC (1:1 v/v)	50	0.01 - 3	243	91 % @ 100 cycles	N/A	N/A	[17]

References

[1] S. Tian, D. Guan, J. Lu, Y. Zhang, T. Liu, X. Zhao, C. Yang and J. Nan, *J. Power Sources*, 2020, **448**, 227572.

[2] R. Hao, H. Lan, C. Kuang, H. Wang and L. Guo, *Carbon*, 2018, **128**, 224–230.

[3] S. Tao, W. Xu, J. Zheng, F. Kong, P. Cui, D. Wu, B. Qian, S. Chen and L. Song, *Carbon*, 2021, **178**, 233–242.

[4] W. Cao, E. Zhang, J. Wang, Z. Liu, J. Ge, X. Yu, H. Yang and B. Lu, *Electrochim. Acta*, 2019, **293**, 364–370.

[5] Y. Sun, H. Xiao, H. Li, Y. He, Y. Zhang, Y. Hu, Z. Ju, Q. Zhuang and Y. Cui, *Chem. - A Eur. J.*, 2019, **25**, 7359–7365.

[6] S. J. R. Prabakar, S. C. Han, C. Park, I. A. Bhairuba, M. J. Reece, K.-S. Sohn and M. Pyo, *J. Electrochem. Soc.*, 2017, **164**, A2012–A2016.

[7] Z. Wu, L. Wang, J. Huang, J. Zou, S. Chen, H. Cheng, C. Jiang, P. Gao and X. Niu, *Electrochim. Acta*, 2019, **306**, 446–453.

[8] C. Gao, Q. Wang, S. Luo, Z. Wang and Y. Zhang, *J. Power Sources*, 2019, **415**, 165–171..

[9] Z. Zhang, B. Jia, L. Liu, Y. Zhao, H. Wu, M. Qin, K. Han, W. A. Wang, K. Xi, L. Zhang, G. Qi, X. Qu and R. V. Kumar, *ACS Nano*, 2019, **13**, 11363–11371.

[10] J. Shan, J.-J. Wang, P. Kiekens, Y. Zhao and J.-J. Huang, *Solid State Sci.*, 2019, **92**, 96–105.

[11] B. Xu, S. Qi, F. Li, X. Peng, J. Cai, J. Liang and J. Ma, *Chinese Chem. Lett.*, 2019, **31**, 217–222.

[12] W.-J. Deng, X.-D. He, L.-M. Zhang, J.-R. Wang and C.-H. Chen, *Energy Technol.*, 2021, **2100644**, 1–6.

[13] X. Yuan, B. Zhu, J. Feng, C. Wang, X. Cai and R. Qin, *Mater. Res. Bull.*, 2021, **139**, 111282.

[14] X. He, J. Liao, Z. Tang, L. Xiao, X. Ding, Q. Hu, Z. Wen and C. Chen, *J. Power Sources*, 2018, **396**, 533–541.

[15] N. Yang, R. Shao, Z. Zhang, M. Dou and J. Niu, *Carbon*, 2021, **178**, 775–782.

[16] K. Zhao, C. Chen, M. La and C. Yang, *Micromachines*, 2022, **13**, 806.

[17] X. Wang, J. Zhao, D. Yao, Y. Xu, P. Xu, Y. Chen, Y. Chen, K. Zhu, K. Cheng, K. Ye, J. Yan, D. Cao, and G. Wang, *J. Electroanal. Chem.*, 2020, **871**, 114272.